

Self-assembly and photophysical studies of an unusual red colored dye which show green fluorescence in cell imaging

VivekshinhKshtriya^[a], Bharti Koshti^[a], Ashadul Haque^[b], Ankit Gangrade^[b], Ramesh Singh, Khashti BallabhJoshi^[c], Sujoy Bandyopadhyay,^[a] Dhiraj Bhatia,^{[b]*} Nidhi Gour^{[a]*}

[a] Department of Chemistry, Indrashil University, Kadi, Mehsana, Gujarat, India; E-mail: nidhi.gour@indrashiluniversity.edu.in; gournidhi@gmail.com

[b] Biological Engineering Discipline, Indian Institute of Technology Gandhinagar, Palaj, Gandhinagar-382355, India; Email: dhiraj.bhatia@iitgn.ac.in

[c] Department of Chemistry, Dr. Hari Singh Gour University, Sagar, Madhya Pradesh, India

Abstract:

We report for the very first time self-assembly of a red color dye 7-Amino-6h-anthra[9,1-cd][1,2]thiazol-6-one (**AAT**), its photophysical properties and its applications in cell imaging. Interestingly, **AAT** show intense red colour in visible light while it shows the orange colour fluorescence under UV light @312nm. Surprisingly, when this dye was used as cell imaging agent it revealed only green fluorescence inside cells and not red. Hence, the photophysical properties of this dye was very intriguing. Further, when self-assembling properties of this dye was examined it revealed formation of tree like branched structures which appeared red both under green and red filter which was again an unexpected

result..Interestingly **AAT** self-assembly also show morphological transition and the branched tree like structures changes to straight fibres as the solvent is changed from DMSO to THF. Hence, the results of self-assembly and cell imaging were contrary to each other and the photophysical properties of this dye is very unusual as compared to conventional dyes. Our future endeavours will aim to understand this anomalous behaviour in greater details in future through various biophysical assays.

Introduction:

Dyes are very important chemical compounds due to their wide range of applications such as textile,¹ plastic industry,² paper industries,³ cell imaging application,⁴ as antiseptic⁵ and also as pharmaceutical drugs.⁶ At present various scaffold-based dyes are available in the market which is based on some specific chromophore that imparts good photophysical properties to the dye, for instance, diazo based chromophore and others like Naphthalene,⁷ Anthraquinone, Indigoid,⁸ coumarin⁹ etc. After azo dyes, anthraquinone based dyes are getting tremendous attention due to its very good electronic conjugation because of the presence of three rings that are fused together. Such chemical structure provide extra planarity and support for the preparation of various dyes. Anthraquinone-based dyes are very important due to their, good lightfastness,¹⁰ brilliance¹¹ and chromophore stability under both acidic and basic conditions.¹² Hence, for these reasons, anthraquinone-based dyes are second most commonly synthesized dyes after the azo dyes.

The 9,10-anthraquinone is the main chromophore unit in anthraquinone based dyes. Substitution with different functional groups lead to changes in photophysical propertiesThe most bathochromic shift is observed when the electron releasing groups are introduced at the alpha position of anthraquinone.Functional groups like -NH₂ and -OH are the most

favourable electron-donating group since they facilitate the donor-acceptor mechanisms operating in chromophore.¹³

Our group has been interested in assessing the self-assembling properties of amino acids,^{14, 15} peptides,^{14, 15} biopolymers,¹⁶⁻¹⁹ and heterocyclic compounds.²⁰⁻²² Recently, we also reported self-assembly of pyridothiazole-based, aggregation-induced emission-enhancement (AIEE) luminogen 4-(5-methoxy-thiazolo[4,5-b]pyridin-2-yl)benzoic acid (PTC1) and its application for the sensitive detection and monitoring of amyloid fibrillation.²⁰ Hence, motivated by our previous studies we were motivated to synthesize a new anthraquinone scaffold which can be effectively used for cell imaging application. Further since our research is based on correlating aggregation properties with the photophysical phenomenon we also wanted to assess the self-assembling behavior of these dyes to assess the molecular mechanism behind its photophysical characteristics.

Herein this manuscript, we report for the very first time self-assembly and photophysical properties of unusual red dye 7-Amino-6h-anthra[9,1-cd][1,2]thiazol-6-one (**AAT**) and its application in cell imaging. The photophysical properties of **AAT** were very unique as it exists in solid form as red color dye while in the solution it forms orange colour and shows orange fluorescence under UV, while in cell imaging studies it reveals green fluorescence only. The self-assembling properties of **AAT** were also exceptional since they reveal branched tree-like red fluorescent structures both under green and red filter and do not reveal any green fluorescence as observed by cell imaging.

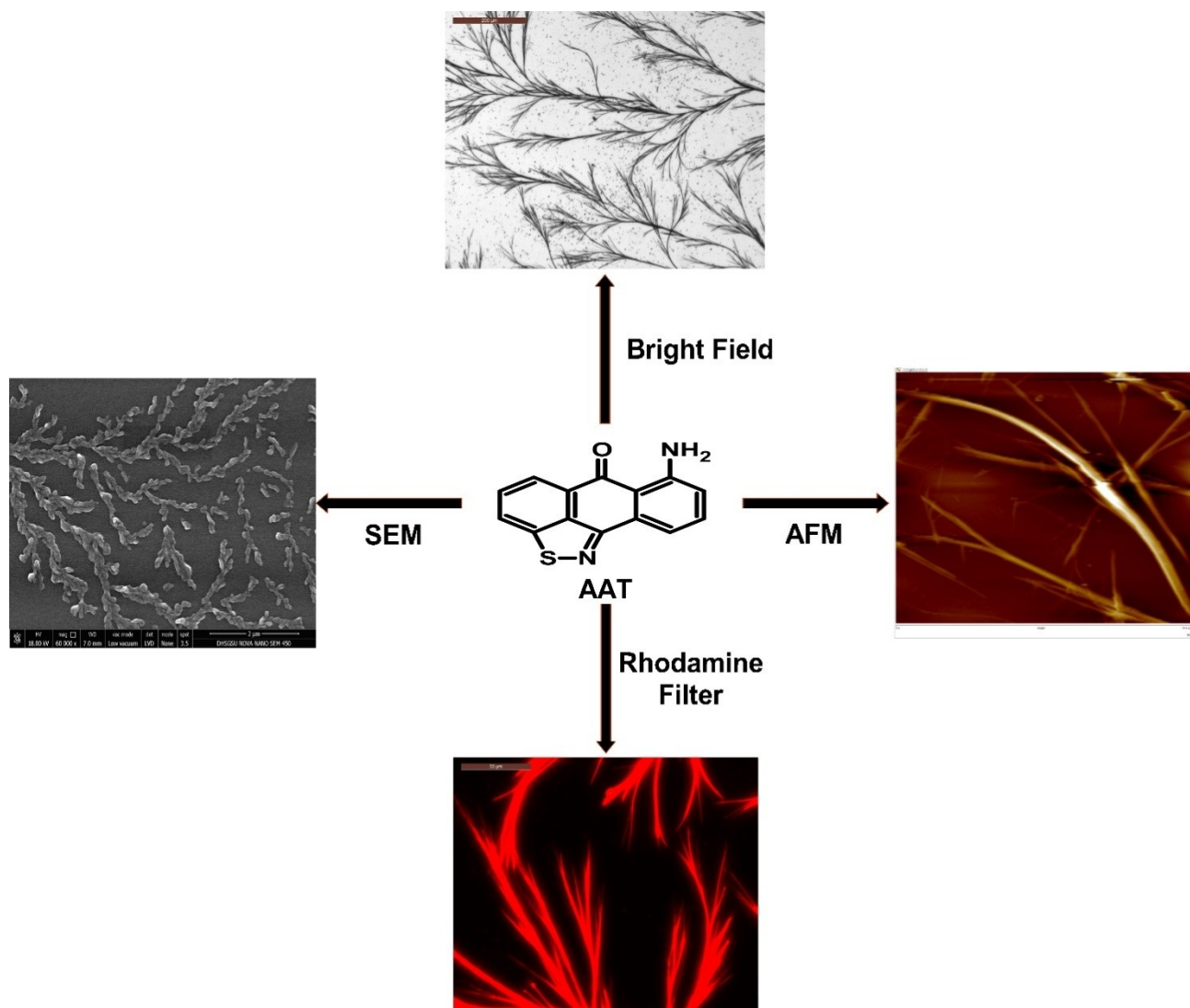
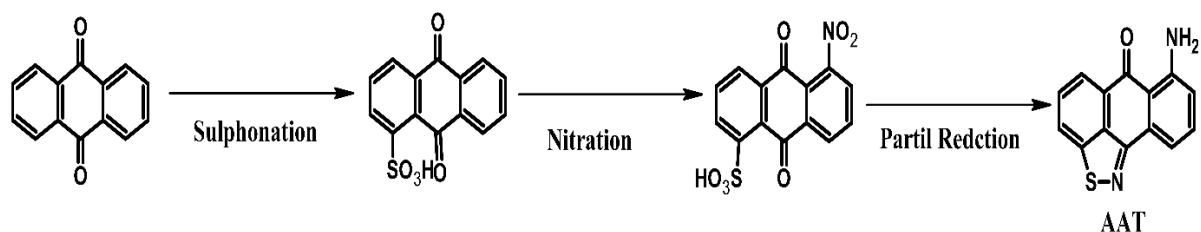


Figure 1. Self-assembled structures formed by AAT and its application in cell imaging.



Scheme 1. Scheme for the synthesis of **AAT**.

7-Amino-6h-anthra[9,1-cd][1,2]thiazol-6-one (**AAT**) was synthesised by reported methodology. In the first step the mono sulphonation was done by using concentrated sulphuric acid which gives the 48% yield, remaining starting material recover which was further use for step-1 preparation. Followed by, in the second step selectively mono nitration has been carried out with use of fuming nitric acid and concentrated sulphuric acid and the final step followed the partial reduction of stage-2 material by using sodium sulfide Na_2S and liquid ammonia under pressure gives the **AAT**.

The as-synthesized **AAT** was characterized by ^1H and ^{13}C NMR spectroscopy and its purity ascertained through analytical HPLC. After complete structural characterization, the self-assembling properties of **AAT** were studied in solution to know the structure formation and to understand its morphology at the supramolecular level. The self-assembling properties of **AAT** molecules were studied at 1mM concentration in DMSO. Notably, **AAT** show branched tree like self-assembled structure in DMSO. Figure 2 illustrated branched tree like self-assembled structures formed by **AAT** in AFM. The SEM image of **AAT** (1mM) at higher magnification reveals beautiful branched tree like morphology. Since the size of assemblies were big, they could also be observed under optical and fluorescence microscope and the tree like assembly appear red under both red and green filter.

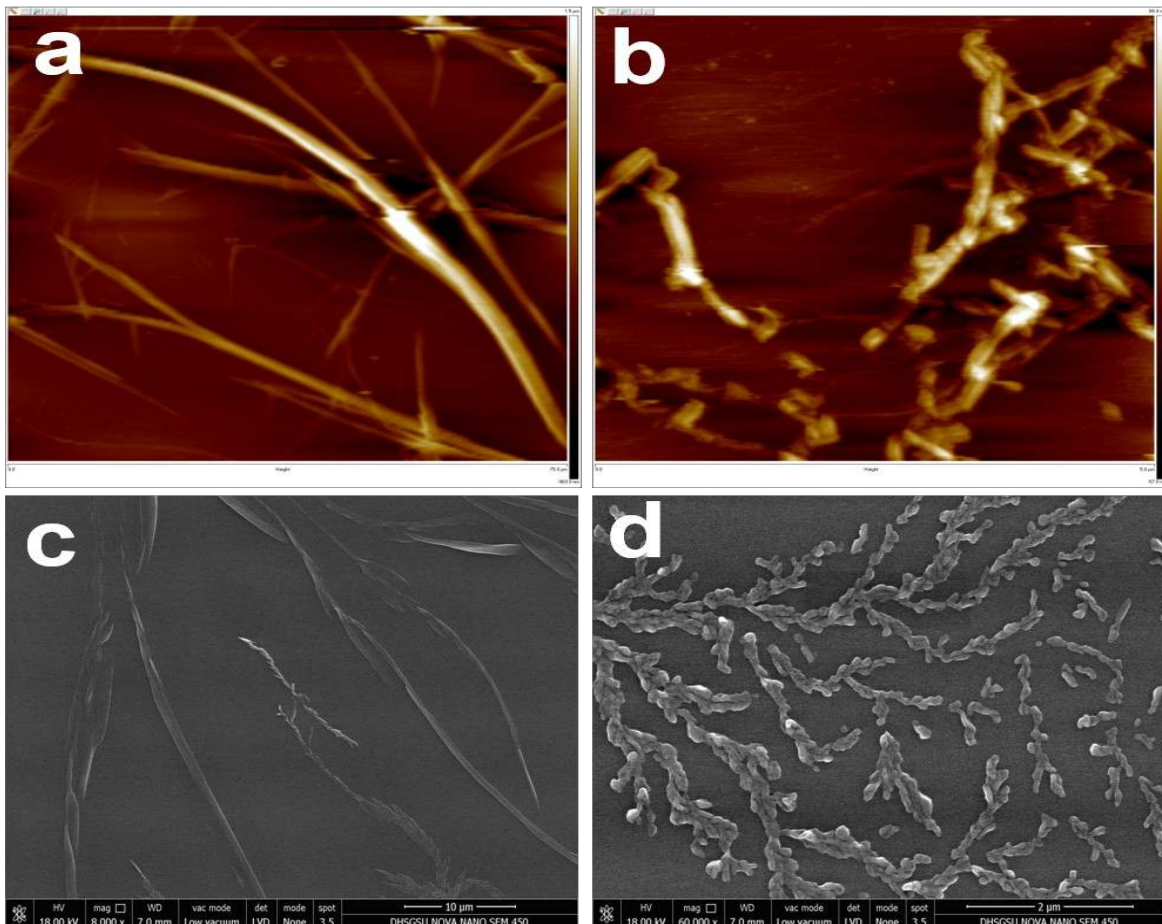


Figure 2: SEM images and AFM images of AAT at 1mM in

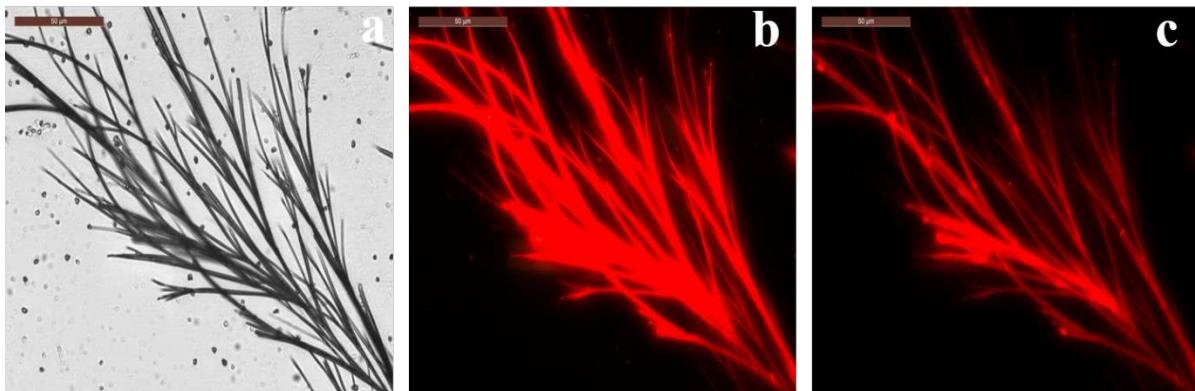


Figure 3. Optical Microscopic images of AAT under bright field, green filter and red filter in DMSO a-c) 1 mM concentration under 40X and scale bar 50μm

Interestingly, when AAT was incubated in non polar solvent like THF the branched tree like assemblies changed to fiber and small fractal like structures. Hence a morphological transition could be observed which suggest crucial role of polarity in the self-assembly.

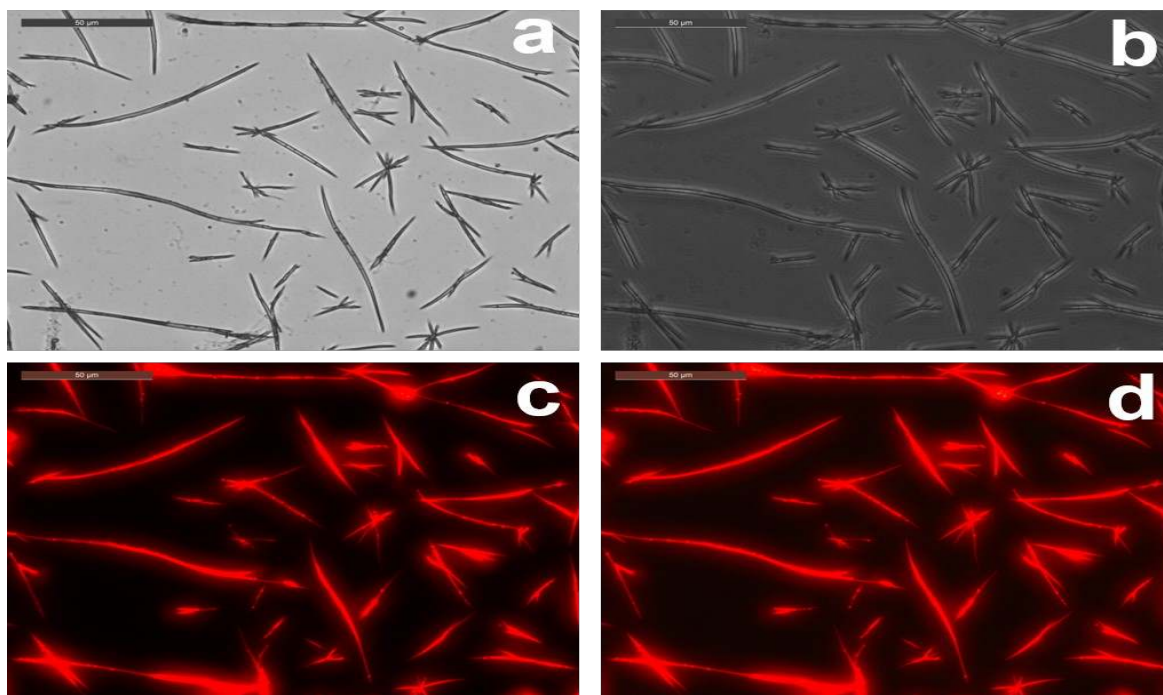


Figure 4. Optical and fluorescence microscopic images of **AAT** in THF. (a) in bright field (b) under phase contrast, (c) under green filter and (d) under red filter at 1 mM concentration under 40X, scale bar 50 μm .

Further, the utility of **AAT** for cell imaging applications were assessed by incubating **AAT** with fixed human. The **AAT**-treated cells were excited with three lasers, and corresponding emission was collected as follows. (excitation 633 nm; emission 643 to 796 nm, excitation 488 nm; emission 500 to 600 nm, excitation 405 nm; emission 415 to 500 nm). Approximately 30 cells were selected from three different images, and their fluorescence intensity was quantified (Figure 10). It can be observed that cells only revealed green fluorescence while minimal fluorescence could be observed in red and blue channel. This observation was very surprising as from self-assembly studies, **AAT** was expected to show red fluorescence.

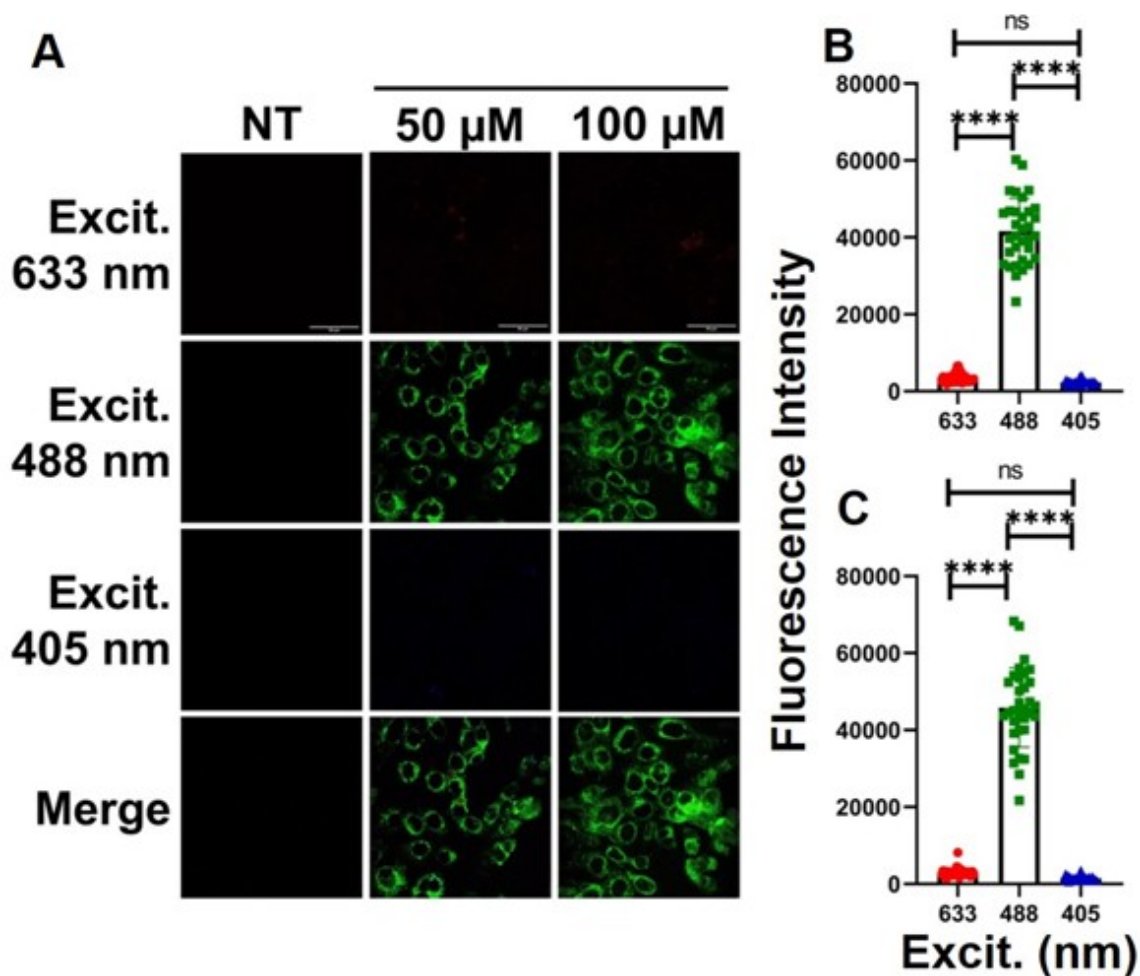


Figure 5. Representative **(A)** confocal microscopy images of human breast cancer cell line (MDA-MB-231) treated with 50 μ M and 100 μ M synthesized **AAT** compound. Fluorescence quantification of **(B)**50 μ M and **(C)**100 μ M concentration **PA** treated cells replotted all three excitation wavelengths. **** Indicates significance level at $P < 0.0001$, * indicates significance level at $P < 0.0329$, and ns indicates no significance between the fluorescence intensities.

Hence, to understand this anomalous photophysical properties of **AAT** in more detail, fluorescence spectra of **AAT** was recorded at 10 μ M concentration. **It was observed that AAT** itself show orange color fluorescence in solution in broad daylight and reveal excitation maxima at 362 and emission maxima at 480 nm which is evince the mirror image spectra obtained in Figure 5. The emission spectra hence corresponded to green fluorescence unlike the orange colored fluorescence which could be seen through the naked eye.

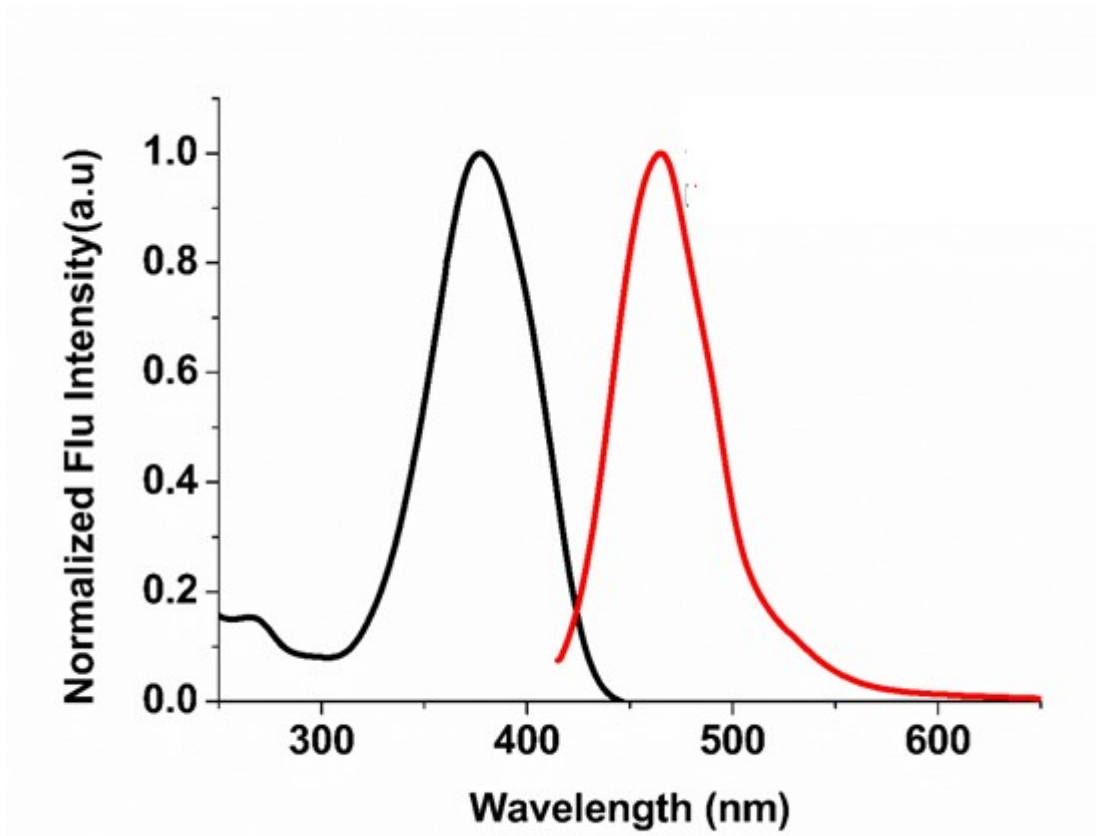


Figure 5. Excitation and Emission spectra of AAT in DMSO at 10uM concentration

Further, to correlate the studies of AAT self-assembly studies, we also recorded fluorescence spectra of AAT by giving excitation 470 which corresponds to green filter of microscope and excitation 538 nm which corresponds to red filter. Under both excitation wavelengths a very broad spectra was obtained which covered red region of the spectra and explains the red fluorescence obtained. (Figure 6)

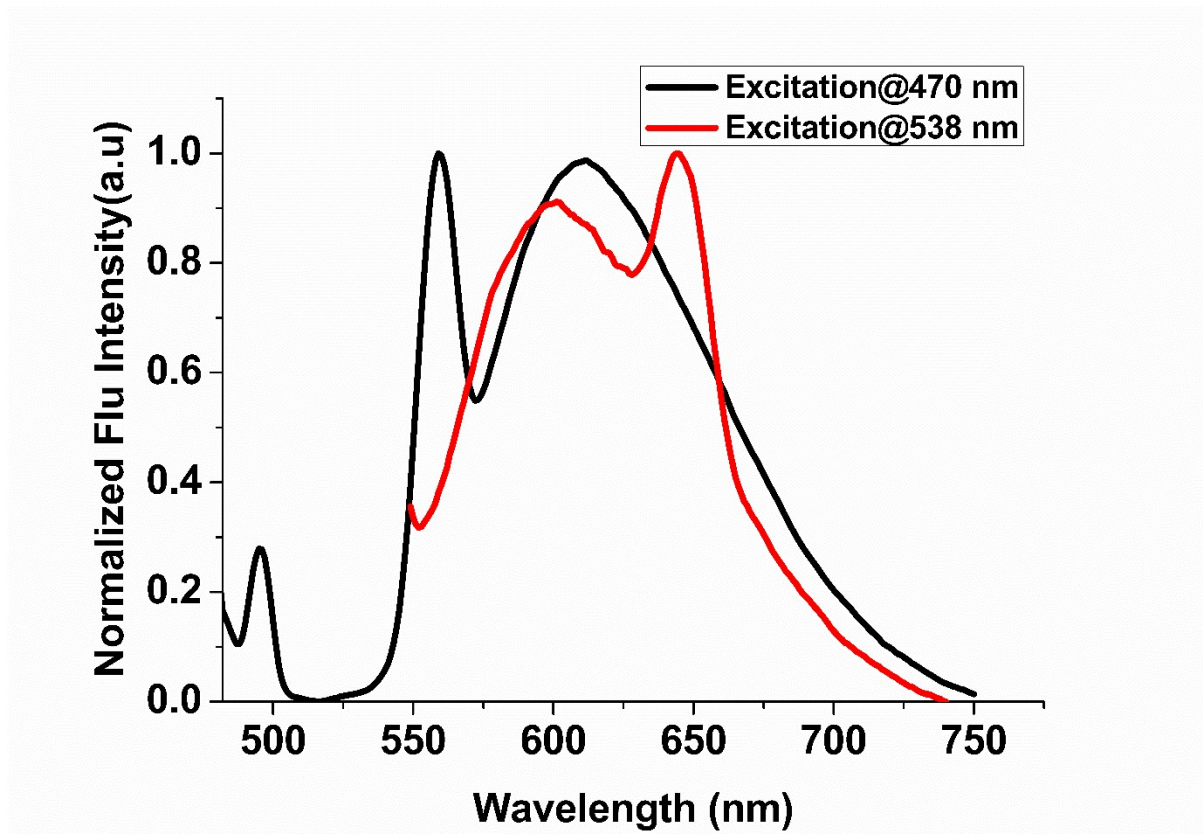


Figure 6: Emission spectra of AAT at 10 uM concentration correspond to the FITC filter and Rhodamine filter in Fluorescence microscopy,

Further, fluorescence spectra of AAT was also recorded by giving the excitation 405, 488 and 633 nm which was used in confocal microscopy for the cell imaging experiments,(Figure 7) The emission spectra in this case appears most prominent under green channel probably because of which the green fluorescence is observed.

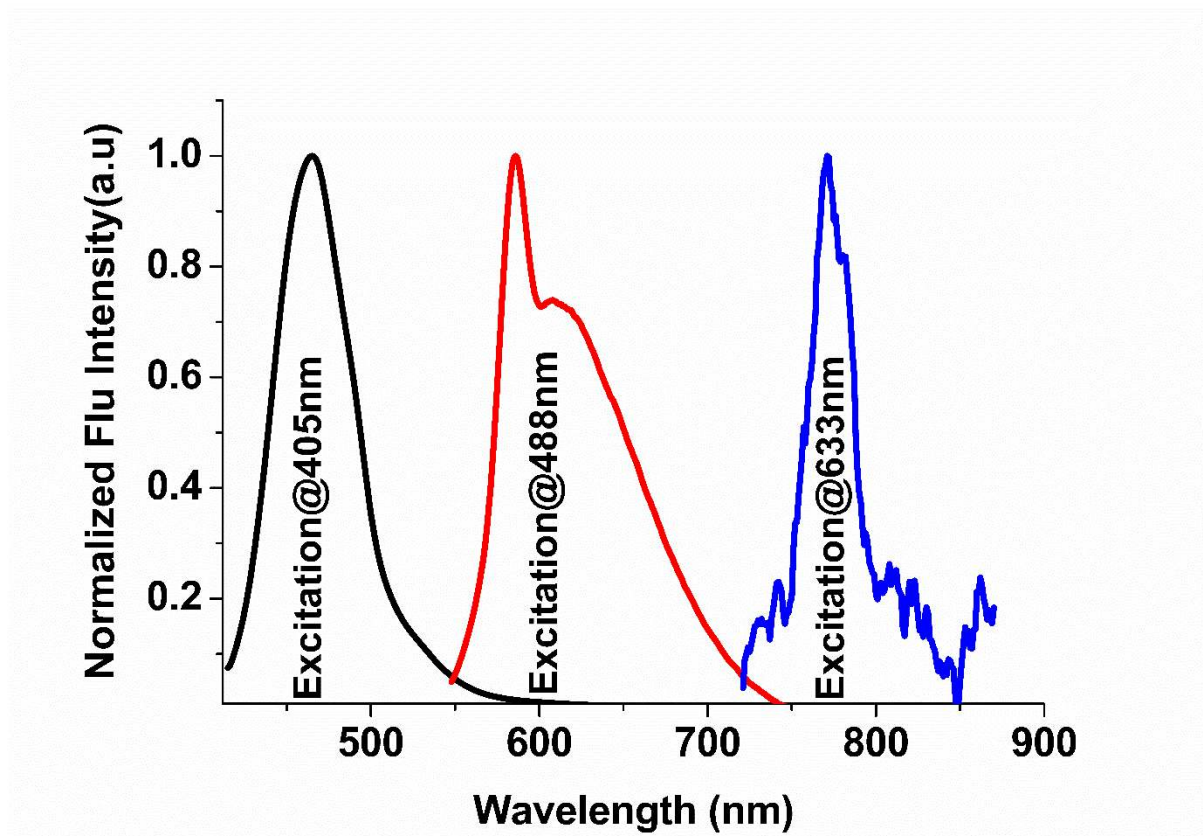


Figure 7: Emission spectra of AAT at 10 μM concentration correspond to the confocal microscopy excitation at 405, 488 and 633 nm.

Materials and method:

Self-assembling properties of AAT

The self-assembly property of AAT was assessed by scanning electron microscopy and optical microscopy, at 1 to 10 mM concentration.

Scanning electron microscopy (FE-SEM)

SEM images were taken using a JSM7600F (Jeol) FE-SEM 450 microscope (the accelerating voltage ranging from 1 to 15 kV). SEM samples were prepared on silicon wafers. A 10 μL AAT of a 1mM solution were dispensed and dried at room temperature. The samples were analyzed without gold coating under a low vacuum.

Atomic Force Microscopy (AFM)

Neat and co-incubated solutions of **AAT** were imaged under an atomic force microscope. The samples were placed on freshly cleaved muscovite mica surfaces followed by imaging with an AFM (INNOVA, ICON analytical equipment, Bruker, operating under the acoustic AC mode (AAC or tapping mode), with the aid of a cantilever (NSC 12(c) from MikroMasch, Silicon Nitride Tip) by NanoDrive version 8 software. The force constant was 2.0 N/m, while the resonant frequency was ~276 kHz. All of the images were taken in the air at rt, with the scan speed of 1.5 lines/sec. The data analysis was done using the nanoscope analysis software. The sample-loaded substrates were dried at dust-free space under a 40W lamp for 30 min followed by high-vacuum drying and subsequently examined under AFM.

Preparation of stock solution:

All the microscopic and spectroscopic studies of **AAT** were done using 10 mM stock solution of **AAT** in DMSO.

UV visible study

The UV-visible spectra have been recorded at 1 to 25 μM concentration by using the 10 mM stock solution of **AAT** in different solvents. The spectra were recorded by using Shimadzu UV-1900 UV-vis spectrophotometer.

Fluorimetric analysis

The excitation and emission spectra of **AAT** were recorded at 10 μM concentration in DMSO. The emission spectra of **AAT** were recorded by giving an excitation wavelength as 375 nm and recorded from 385 to 800 nm. Similarly, the excitation spectra were recorded from 200 to 800 nm, where the maximum emission wavelength (λ_{em}) was found to be 462 nm. The experiment has been performed on Jasco spectrofluorometer FP 8300.

Solvent dependent study of AAT

The solvent dependent study has been done at 10 μ M concentration by using 10 mM stock solution in DMSO through UV-visible and Spectrofluorometer instrument in DMSO, THF, Water, Hexane, Etoc, IPA, chloroform, ACN, MeOH, Ethanol, Acetone,

Cytotoxic assay:

Cell imaging:

Human breast cancer (MDA-MB-231) cells were grown in DMEM cell culture media supplemented with 10% FBS and 1% antibiotic in a 5% CO₂ incubator. First, the cells were seeded onto a glass coverslip and fixed with 4% paraformaldehyde. Later the fixed cells were treated with 50 μ M and 100 mM AAT for 15 min at room temperature. The coverslips were then mounted on a glass slide, and images were captured in Leica confocal microscope.

Conclusions.

In conclusion, we have reported self-assembly and photophysical properties of 7-Amino-6h-anthra[9,1-cd][1,2]thiazol-6-one (**AAT**). **AAT** self-assembles to branched tree like morphologies in DMSO and these assemblies show red fluorescence in both green and red filters. These morphologies changes to fiber like structures in THF which also reveal red fluorescence. . However, when the utility of **AAT** is assessed as a cell imaging agent in human breast cancer cell lines (MDA-MB-231) the cells revealed green emission and no red fluorescence. These results were very surprising and show anomalous behavior of this dye. We have tried to explain this unusual behavior through fluorescence spectroscopy of **AAT** in varying excitation wavelengths. However, more studies need to be pursued to find the exact reasoning for this anomaly.

Reference:

1. Ferreira, E. S.; Hulme, A. N.; McNab, H.; Quye, A., The natural constituents of historical textile dyes. *Chemical Society Reviews* **2004**, 33 (6), 329-336.
2. Christie, R. M., Pigments, dyes and fluorescent brightening agents for plastics: An overview. *Polymer international* **1994**, 34 (4), 351-361.

3. Guohui, C. G. L. S. X.; Hongwei, T. A. Z., Characteristics and Application Technology of Dyes Used in Paper Industry [J]. *Dyestuff Industry* **2002**,4.
4. MacNevin, C. J.; Gremyachinskiy, D.; Hsu, C.-W.; Li, L.; Rougie, M.; Davis, T. T.; Hahn, K. M., Environment-sensing merocyanine dyes for live cell imaging applications. *Bioconjugate chemistry* **2013**,24 (2), 215-223.
5. Volwiler, E. H., Medicinals and dyes. *Industrial & Engineering Chemistry* **1926**,18 (12), 1336-1337.
6. Wainwright, M., The use of dyes in modern biomedicine. *Biotechnic & Histochemistry* **2003**,78 (3-4), 147-155.
7. Mathauer, K.; Frank, C. W., Naphthalene chromophore tethered in the constrained environment of a self-assembled monolayer. *Langmuir* **1993**,9 (11), 3002-3008.
8. Petermayer, C.; Dube, H., Indigoid photoswitches: visible light responsive molecular tools. *Accounts of chemical research* **2018**,51 (5), 1153-1163.
9. Katerinopoulos, H. E., The coumarin moiety as chromophore of fluorescent ion indicators in biological systems. *Current pharmaceutical design* **2004**,10 (30), 3835-3852.
10. Shan, B.; Tong, X.; Xiong, W.; Qiu, W.; Tang, B.; Lu, R.; Ma, W.; Luo, Y.; Zhang, S., A new kind of H-acid monoazo-anthraquinone reactive dyes with surprising colour. *Dyes and Pigments* **2015**,123, 44-54.
11. Ren, S.; Guo, J.; Zeng, G.; Sun, G., Decolorization of triphenylmethane, azo, and anthraquinone dyes by a newly isolated *Aeromonas hydrophila* strain. *Applied microbiology and biotechnology* **2006**,72 (6), 1316-1321.
12. Le Comte, A.; Brousse, T.; Bélanger, D., Simpler and greener grafting method for improving the stability of anthraquinone-modified carbon electrode in alkaline media. *Electrochimica Acta* **2014**,137, 447-453.
13. Hunger, K., Industrial dyes: chemistry, properties, applications. **2007**.
14. Gour, N.; Kanth P, C.; Koshti, B.; Kshtriya, V.; Shah, D.; Patel, S.; Agrawal-Rajput, R.; Pandey, M. K., Amyloid-like structures formed by single amino acid self-assemblies of cysteine and methionine. *ACS chemical neuroscience* **2018**,10 (3), 1230-1239.
15. Koshti, B.; Singh, R.; Kshtriya, V.; Walia, S.; Bhatia, D.; Gour, N., Amyloid like aggregates formed by the self-assembly of proline and Hydroxyproline. **2021**.
16. Gour, N.; Mondal, S.; Verma, S., Synthesis and self-assembly of a neoglycopeptide: morphological studies and ultrasound-mediated DNA encapsulation. *Journal of Peptide Science* **2011**,17 (2), 148-153.
17. Gour, N.; Barman, A. K.; Verma, S., Controlling morphology of peptide-based soft structures by covalent modifications. *Journal of Peptide Science* **2012**,18 (6), 405-412.
18. Gour, N.; Verma, S., Bending of peptide nanotubes by focused electron and ion beams. *Soft Matter* **2009**,5 (9), 1789-1791.
19. Gour, N.; Kedracki, D.; Safir, I.; Ngo, K. X.; Vebert-Nardin, C., Self-assembling DNA-peptide hybrids: morphological consequences of oligonucleotide grafting to a pathogenic amyloid fibrils forming dipeptide. *Chemical Communications* **2012**,48 (44), 5440-5442.
20. Gour, N.; Kshtriya, V.; Gupta, S.; Koshti, B.; Singh, R.; Patel, D.; Joshi, K. B., Synthesis and Aggregation Studies of a Pyridothiazole-Based AIEE Probe and Its Application in Sensing Amyloid Fibrillation. *ACS Applied Bio Materials* **2019**,2 (10), 4442-4455.
21. Gour, N.; Kshtriya, V.; Koshti, B.; Gangrade, A.; Haque, A.; Bhatia, D., Synthesis and Characterization of the Fluorescent Self-Assembled Structures Formed by Benzothiazolone Conjugates and Applications in Cellular Imaging. **2021**.
22. Kshtriya, V.; Koshti, B.; Gour, N., A New Azo Dye Based Sensor for Selective and Sensitive Detection of Cu (II), Sn (II), and Al (III) Ions. **2021**.

